24th COBEM - 2017

24th ABCM International Congress of Mechanical Engineering
December 3-8, 2017, Curitiba, PR, Brazil

COBEM-2017-0139
WHAT DOES LINEAR INSTABILITY TELL US ABOUT AIRFOIL TONAL NOISE?

Daniel Rodríguez
Graduate Program in Mechanical Engineering (PGMEC), Universidade Federal Fluminense, Brazil
danielrodriguez@id.uff.br

Elmer M. Gennaro
São Paulo State University (UNESP), Campus of São João da Boa Vista, Brazil
elmer.gennaro@sjbv.unesp.br

Walter Arias Ramírez
William R. Wolf
University of Campinas, Brazil
walter.arias.ramirez@gmail.com, wolf@fem.unicamp.br

Abstract. *Several studies spanning since the 1970s to the present, considering turbulent flows at realistic conditions for aircraft flight, have amassed evidence on the dominance of a far-field tonal noise, usually associated with vortex-shedding from the trailing edge. Furthermore, the appearance of multiple tones has been documented for increasing values of the angle of attack and Mach number, which exhibit a ladder-like pattern in terms of the variation of the frequencies with increasing free-stream velocity. Different explanations have been suggested for the origin of the (i) single tone, (ii) multiple tones evenly spaced in frequency and (iii) the ladder-like behavior as free-stream is increased, most of them based on the instability properties of the underlying flow. This contribution presents a comprehensive study of the linear mechanisms possibly acting on a NACA 0012 airfoil, at different Reynolds numbers, angles of attack and Mach numbers. Local and global analyses are performed, on the purpose of extracting all the possible information and eliminating biases associated to the choice of a single methodology. In this sense, ad hoc absolute/convective, multiple-scales analyses, parabolized stability equations and biglobal stability analyses are applied and combined, with the objective of ascertaining if and how airfoil tonal noise can be fully explained, characterized and predicted by linear instability mechanisms. A positive answer to this question would have a tremendous impact regarding flow control and airfoil noise reduction.*

Keywords: *Airfoil noise, Flow instability, Aero-acoustics, Computational Fluid Dynamics*

1. INTRODUCTION

The understanding of trailing edge noise is an overriding concern for the design of low-noise aerodynamic shapes including high-lift components, wind turbine blades, fans and even car roof racks. Brooks *et al.* (1989) identify vortex shedding due to laminar boundary layer instabilities and blunt trailing edges as sources of airfoil self-noise. Wolf *et al.* (2012a, 2013, 2012b) performed numerical investigations of airfoil self-noise generation for turbulent flows past NACA0012 and DU96 airfoils showing that tonal noise may appear in far-field acoustic predictions for blunt trailing edges even in the presence of fully turbulent boundary layers. The presence of tonal noise would then depend on the ratio between the trailing edge thickness and the boundary layer displacement thickness.

Several pioneering studies of airfoil noise were conducted in the 1970s in order to examine airfoil tonal noise generation. These investigations showed that discrete tones are emitted from isolated airfoils at specific flow conditions (Smith *et al.* (1970); Clark (1971); Hersh and Hayden (1971); Longhouse (1977)). Such findings triggered some of the first systematic and detailed studies of airfoil tonal noise (Paterson *et al.* (1973); Tam (1974); Fink (1975); Fink *et al.* (1976); Arbey and Bataille (1983)). Paterson *et al.* (1973) performed noise measurements from symmetric NACA airfoils for a Reynolds number range between 10^5 and 10^6 and various angles of attack; their results showed the existence of multiple tones in a ladder-like structure pattern in terms of frequency and free-stream velocity. Furthermore, they measured spanwise surface pressure fluctuations on the airfoils and found strong correlation over a considerable extent along the airfoil surface. This indicated that the flow phenomenon associated with airfoil tonal noise generation could be modeled as two dimensional.

Another theory for the power law observed by Paterson was proposed by Fink (1975). He assumed that the discrete

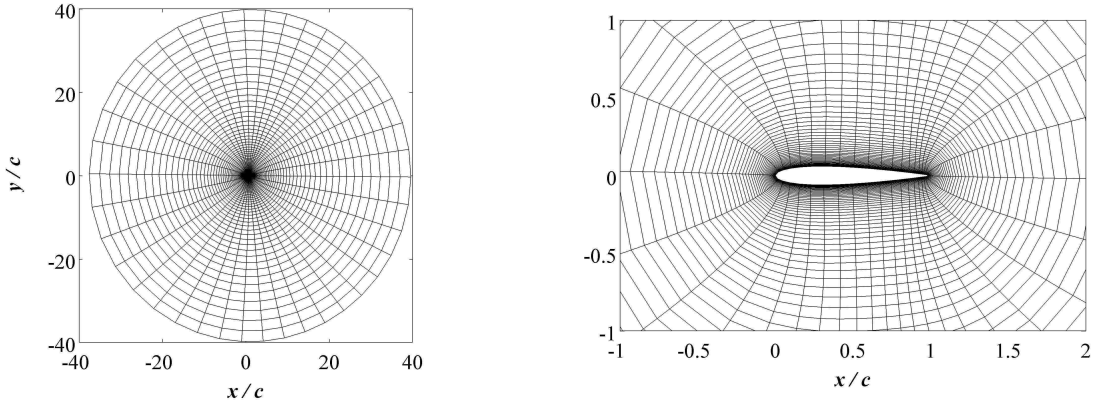

Figure 1. O-type mesh used in the direct numerical simulations and global eigenmode analyses. One on each 10 points is shown on each direction on the purpose of visualization. Left: Complete computational domain used in the DNS. Right: Zoom on the airfoil.

frequencies were linked to the laminar boundary-layer developing along the pressure side of the airfoil. Arbey and Bataille (1983) repeated the experimental studies from Paterson in an open wind tunnel for three different NACA airfoils and showed that the noise spectrum was composed of a broadband contribution with a main tonal peak plus a set of equidistant secondary tones.

Recently, Desquesnes *et al.* (2007) performed 2D direct numerical simulations (DNS) of flows past a NACA0012 airfoil for Reynolds numbers 1×10^5 and 2×10^5, and angles of attack of 2 and 5 degs. Their results presented the multiple tonal peaks consistent with the experimental observations from Arbey and Bataille (1983). Kurotaki *et al.* (2008), Chong and Joseph (2013) and Plogmann *et al.* (2013) also found multiple tones in their experimental results and the so-called ladder-like structure pattern. Related studies were conducted numerically by Jones and Sandberg (2011) and Tam and Ju (2011). An in-depth theoretical study of the physical causes of the ladder-like structure of tones was done by Fosas de Pando *et al.* (2014), combining numerical simulations with linear global stability analysis, for a NACA0012 at Reynolds number 2×10^5 and Mach number 0.4. These latter studies suggest that tonal noise is related to a feedback mechanism established between the boundary-layer instability and the acoustic waves. The trailing edge, being responsible for the emission and scattering of acoustic waves, would play a decisive role in the selection of the tonal frequencies observed both in experiments and simulations. Modifications of the trailing edge geometry, e.g. replacing the sharp edge characteristic of the NACA family with a blunt one, are possible means of altering the feedback mechanism and could be exploited in order to achieve overall noise reductions.

The current work presents a study of the instability properties of flows past a NACA0012 airfoil with blunt trailing edge with different Reynolds and Mach numbers. Weakly non-parallel stability analysis, parabolized stability equations and global eigenmode analyses are applied, in order to shed light on the mechanisms responsible for the main and secondary tones observed in direct numerical simulations.

2. FLOW CONFIGURATIONS AND DIRECT NUMERICAL SIMULATIONS

The present contribution considers the same geometries, flow configurations and set of parameters that are studied by Arias-Ramirez and Wolf (2015, 2016). Two modifications of the NACA0012 airfoil geometry are defined, in which the trailing edge (TE) is rounded and the airfoil chord c reduced accordingly. The geometry labeled TE1 corresponds to a TE radius of $0.004c$ and a total chord $c = 0.98$; the geometry labeled TE2 has radius $0.025c$ and chord $c = 0.8$. For each geometry, two angles of attack (AoA), AoA = 0 and 3 degrees and three Mach numbers $Ma = 0.1, 0.2$ and 0.3 are simulated for different values of the Reynolds number Re.

Direct numerical simulations (DNS) are performed by solving the non-dimensional 2D compressible Navier-Stokes equations in general curvilinear coordinates. Length, velocity, density and pressure are non-dimensionalized by the airfoil chord c, free-stream speed of sound a_∞, free-stream density ρ_∞ and $\rho_\infty a_\infty^2$, respectively. A sixth-order accurate compact finite differences scheme (Nagarajan *et al.* (2003)) is employed for the spatial discretization of the governing equations, together with a high wavenumber compact filter to damp numerical instabilities arising from mesh non-uniformities and interpolation at grid interfaces. Time integration is carried out by the fully implicit second-order scheme of Beam and Warming (1978) in the near-wall region, while a third-order Rung-Kutta scheme is used in regions far away from solid boundaries. No-slip adiabatic wall boundary conditions are applied along the solid surface and characteristic plus sponge boundary conditions are applied in the far field to minimize wave reflections. The acoustic far-field is calculated using a

hybrid approach which couples the DNS for the computation of the near-field sources and the Ffowcs Williams - Hawkings (KW-H) equation (Ffowcs Williams and Hawkings (1969)) for the noise radiation. Further details on the numerical code and its validations can be found elsewhere (Wolf *et al.* (2012a, 2013); Arias-Ramirez and Wolf (2016)).

Two O-type meshes are used in the simulations. The first has 400×700 points in the azimuthal direction and normal directions respectively and is employed for the lower Reynolds number flow calculations at $Re = 5000$ and 10000. The second mesh has 400×900 points and it is used for the moderate Reynolds numbers $Re = 50000$ and 100000. Figure 1 illustrates the structured mesh topology and clustering on the airfoil surface.

3. LINEAR INSTABILITY ANALYSES

Linear instability analyses consider the temporal, spatial and spatio-temporal evolution of disturbances of linearly-small amplitude superimposed to a time-invariant base flow. Formally, the state vector $\mathbf{q} = [\rho, u, v, p, T]^T$ comprising all the fluid variables of interest is decomposed into the time-invariant base flow $\bar{\mathbf{q}}$ and time-dependent fluctuations or disturbances $\mathbf{q}'$. For the 2D flows around airfoils considered here

$$\mathbf{q}(x, y, t) = \bar{\mathbf{q}}(x, y) + \varepsilon \mathbf{q}'(x, y, t), \tag{1}$$

where $\varepsilon \ll 1$ denotes the small disturbance amplitude. Substitution of the previous flow decomposition in the governing (continuity, Navier-Stokes and energy) equations and subtraction of the $O(1)$ corresponding to the time-invariant base flow results into the disturbance-form Navier-Stokes equations, governing the fluctuations. Furthermore, the non-linear terms ($O(\varepsilon^2)$) are neglected based on the smallness of the disturbance amplitude, yielding to the linearized compressible Navier-Stokes equations. In general terms, a base flow is unstable when the amplitude of a random disturbance increases without limit after its introduction, until finite disturbance amplitudes are attained and non-linearities become relevant. Stable flows, on the other hand, are those for which any given disturbance decays asymptotically to vanishing amplitudes, and the flow variables return to the undisturbed base flow. Instability analyses done herein are (i) linear and (ii) based on the mean (time-averaged) flow, rather than on a steady solution of the equations. In many unstable flows at near-critical conditions, stability analyses of the mean flow can be used to study the physical mechanisms for the onset of unsteadiness, together with their associated frequencies, growth rates and spatial structures. However, it must be kept in mind that non-linearities responsible for the disturbance growth saturation have the potential to modify frequencies and structures, as well as to produce additional oscillations.

In the following subsections, different *ad hoc* methodologies for the linear instability analysis are employed in the study of the mechanisms responsible for the different features observed in the far-field sound spectra.

3.1 Self-sustained wake oscillations

The near-field pressure spectra for AoA = 0 degrees and the lowest Reynolds numbers ($Re = 50000$ for TE1 and $Re = 50000$ and $Re = 100000$ for TE2 and lowest Mach numbers) is dominated by a single tonal frequency plus its harmonics. The fundamental frequency grows nearly linearly with the Mach number, which in the present dimensionless form is related to the inflow velocity. Inspection of the instantaneous velocity field shows the formation of vortical structures in the vicinity of the trailing edge region, that are shed in the wake forming the well-known Von Karman vortex street. This suggests the single tone to be associated to the vortex shedding, and the use of instability analyses on the wake region to predict (i) whether or not a global oscillator exists, that leads to a self-sustained vortex shedding, and (ii) the fundamental tone frequency.

As was demonstrated by Chomaz *et al.* (1988); Huerre and Monkewitz (1990), self-sustained oscillations of the flow can be predicted by the linear stability analysis of the local, flow-transverse velocity profiles. Considering the base flow to be locally-parallel at each x-coordinate, the streamwise variations of $\bar{\mathbf{q}}$ are neglected and the flow decomposition (1) is transformed into a series of local (for each X coordinate) problems

$$\mathbf{q}(y, t; X) = \bar{\mathbf{q}}(y; X) + \varepsilon \hat{\mathbf{q}}(y; X) \exp\left[\mathrm{i}(\alpha(X)x - \omega)t\right] + c.c., \tag{2}$$

where Laplace transforms have been applied to the x-direction and time, resulting in the introduction of the complex wavenumber $\alpha = \alpha_r + \mathrm{i}\alpha_i$ and circular frequency $\omega = \omega_r + \mathrm{i}\omega_i$; *c.c.* stands for the complex conjugate, required for the result to be a real quantity. Substitution of this Ansatz in the governing equations results into a series of complex eigenvalue problems (EVP), one for each X coordinate, which can be recast as generalized matrix EVP either for the frequency or the wavenumber. In the so-called temporal problem the wavenumber α is prescribed, and complex frequencies ω are recovered as eigenvalues. In the spatial problem the frequency ω is prescribed and the wavenumbers α are the eigenvalues. Disturbance oscillations in the $x - t$ plane and growth or decay are determined respectively by the real and imaginary parts of α and ω. The real part of α is a streamwise wavelength, while the real part of ω corresponds, in the present dimensionless form, to the Helmholtz number He. A positive ω_i corresponds to an exponential growth in time, and thus to flow instability. A negative α_i corresponds to an exponential growth along x.

Table 1. Comparison between the peak frequency in the DNS near-field spectra He, the frequency predicted by the linear global oscillator analysis ω_r, the frequency for the maximum amplification of boundary-layer disturbances ω_{max} and its corresponding N factor.

Geometry	AoA	Re	Ma	DNS - He	GO - ω_r	PSE - ω_{max}	PSE - N_{max}
TE1	0	50000	0.1	2.920	2.613	2.464	0.85
TE1	0	50000	0.2	5.873	5.248	4.993	2.61
TE1	0	50000	0.3	8.493	7.681	7.553	3.97
TE1	0	100000	0.1	3.578	3.233	3.520	3.13
TE1	0	100000	0.2	7.295	6.512	7.222	5.26
TE1	0	100000	0.3	10.932	10.946	13.012	9.33
TE1	3	50000	0.1	2.816	3.221	–	–
TE1	3	50000	0.2	6.552	6.698	–	–
TE1	3	50000	0.3	9.206	10.024	–	–
TE1	3	100000	0.1	3.571	4.027	–	–
TE1	3	100000	0.2	9.589	8.154	–	–
TE1	3	100000	0.3	12.130	12.021	–	–
TE2	0	50000	0.1	1.940	1.718	STB	0.00
TE2	0	50000	0.2	3.843	3.446	STB	0.00
TE2	0	50000	0.3	5.658	5.127	STB	0.00
TE2	0	100000	0.1	2.151	1.863	STB	0.00
TE2	0	100000	0.2	4.226	3.722	11.101	0.01
TE2	0	100000	0.3	7.121	6.021	16.201	0.70

From either the temporal or the spatial frameworks, an implicit relation between α and ω is obtained for each X-location, referred to as the dispersion relation $\mathcal{D}(\alpha, \omega, X) = 0$. The existence of self-sustained oscillations requires of the existence of a spatial region (in X) in which absolute instability occurs, i.e. unstable waves propagate upstream. A global oscillator can appear then, in which the fluctuations at different sections X are synchronized and described by a complex global frequency ω_g. The process for the determination of the global frequency consists of (i) determining the absolute frequency for each section X, $\omega_0(X)$, and (ii) determining the global frequency based on $\omega_0(X)$. The absolute frequency ω_0 is the one associated to disturbances with propagation speed equal to zero, and is determined at each X by the dispersion relation and the saddle-point condition

$$\frac{\partial \omega}{\partial \alpha} = 0, \quad \Rightarrow \quad \omega_0(X) \tag{3}$$

If the imaginary part of the absolute frequency $\omega_{0,i} > 0$, then there exist waves that propagate upstream with temporal growth and the flow is said to be (locally) absolutely unstable. This upstream influence of the disturbances can give rise to self-excited oscillations of the flow. One criterion for the determination of the global oscillation frequency was proposed by Chomaz *et al.* (1988), and is based on the complex X-plane saddle-point condition

$$\frac{\partial \omega_0}{\partial X} = 0, \quad \Rightarrow \quad \omega_g. \tag{4}$$

Finally, a global oscillator occurs when the imaginary part of the global frequency, $\omega_{g,i} > 0$, and the (linear) oscillation frequency is given by $\omega_{g,r}$. Weakly non-linear theoretical developments and comparisons with experiments show that the actual oscillation frequencies observed in saturated conditions, once the disturbance growth has ceased, are smaller (up to 15% reduction) but comparable to that predicted by the linear global oscillator (Huerre and Monkewitz (1990)).

The application of this methodology to the DNS mean flows predicts the existence of a global oscillator in all cases. Table 1 compares the oscillation frequency predicted by the linear oscillator analysis with the peak frequency in the DNS near-field pressure spectra.

3.2 Spatial growth of boundary-layer instability waves

The origin of dominant frequencies in the near-field pressure spectra has been suggested, alternatively to the vortex shedding associated with the near wake, to the spatial amplification of convectively unstable by absolutely stable instability waves within the boundary layer. This possibility is particularly relevant to relatively high Reynolds numbers and wind-tunnel experiments, in which a certain level of external turbulence is always present, and through a complex receptivity

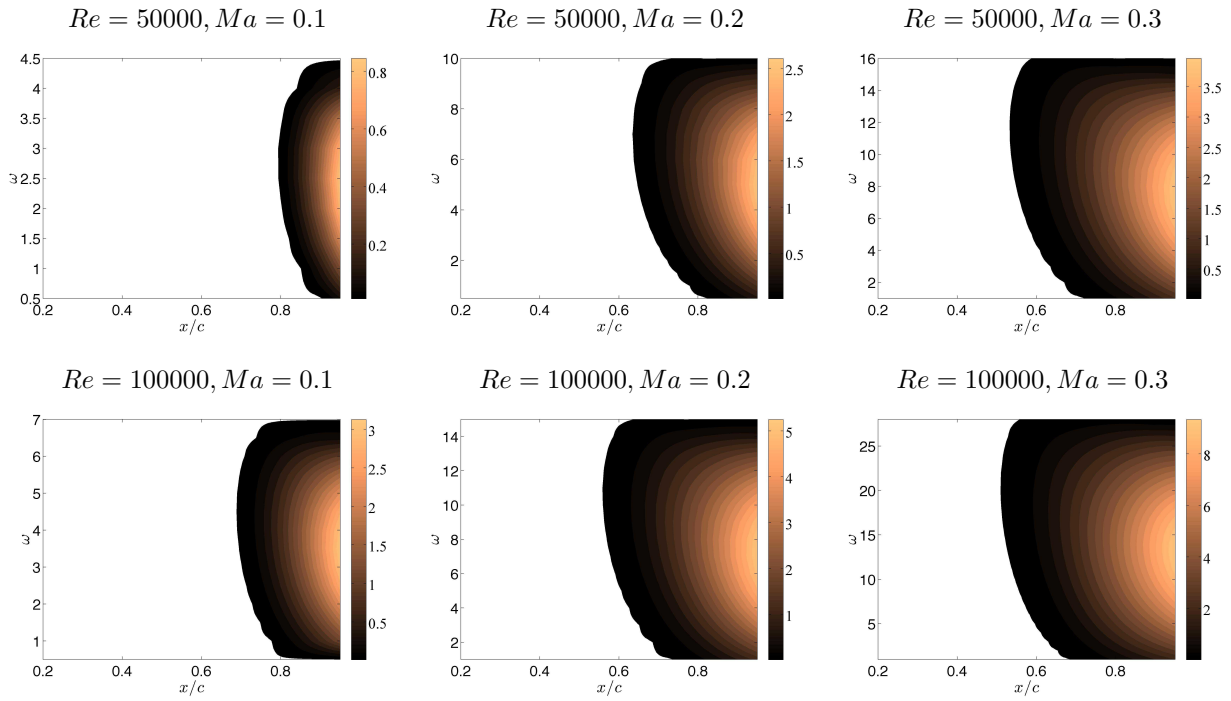

Figure 2. Spatial amplification of boundary-layer instability waves computed by PSE, as contours of the N-factor. TE1 geometry at AoA = 0 deg., $Re = 50000$ (top) and $Re = 100000$ (bottom), and $Ma = 0.1$ (left), 0.2 (middle) and 0.3 (right).

process localized in the vicinity of the airfoil leading edge, gives rise to the so-called Tollmien-Schlichting waves. Towards the aft portion of the airfoil, the boundary layer is subjected to an adverse-pressure-gradient that leads to an important boundary-layer thickness growth and eventually to separation, close to the trailing edge. The inflectional nature of the decelerated boundary-layer acts by strongly destabilizing the disturbance waves, potentially leading to vortex formation even upstream of the trailing edge.

The spatial amplification of boundary-layer instability waves is studied here using the parabolized stability equations (PSE). PSE are based on the weakly non-parallel flow approximation, in which the base flow properties are allowed to have a mild variation along the streamwise direction. A separation in scales is introduced then for the streamwise direction, in which X stands for the slow scale, in which the variations of the base flow are relevant, while instability wavelengths are assumed to be measurable in the short scale x. This allows for the introduction of the Ansatz

$$\mathbf{q}(x,y,t) = \bar{\mathbf{q}}(X,y) + \varepsilon\hat{\mathbf{q}}(X,y)\exp\left[\mathrm{i}(\int_x \alpha(X)\mathrm{d}X - \omega)t\right] + c.c. \tag{5}$$

in which both the disturbance shape function $\hat{\mathbf{q}}$ and wavenumber α are allowed to vary on the long scale X. Substitution of this decomposition on the linearized governing equations, and neglecting the second-order derivatives on x for the shape function allows to recast the equations as a parabolic marching one for each frequency. For given conditions at an initial cross section, PSE integration computes the spatial structure, wavenumber and amplification along the boundary layer. More details can be found in the classic references (Bertolotti *et al.* (1992); Herbert (1997)).

Taking advantage of the body-fitted structured mesh employed in the DNS, the region of the flow field surrounding the wall and comprising the boundary layer is extracted. The chord-length coordinate measured from the leading edge and the wall-normal coordinate are used in the PSE. The non-parallelism of the mean flow was quantified by comparing the peak tangential and normal velocity components at each chord position, which were found to be below 1% except for the immediate vicinity of the leading and trailing edges. The integration of the PSE equations was initiated at $x/c = 0.2$, were the boundary layer is very thin and instability waves for all frequencies are damped. The initial wavenumber and shape function were obtained from a locally-parallel analysis, in which the (stable) Tollmien-Schlichting eigenmode was chosen. As the integration proceeds towards the trailing edge, the instability waves become unstable for a bounded frequency range, as shown in figure 2 for some representative cases. The spatial amplification is quantified in terms of the N-factor, defined as

$$N = -\int_{x_n}^{x} \alpha_i(X)\mathrm{d}X \tag{6}$$

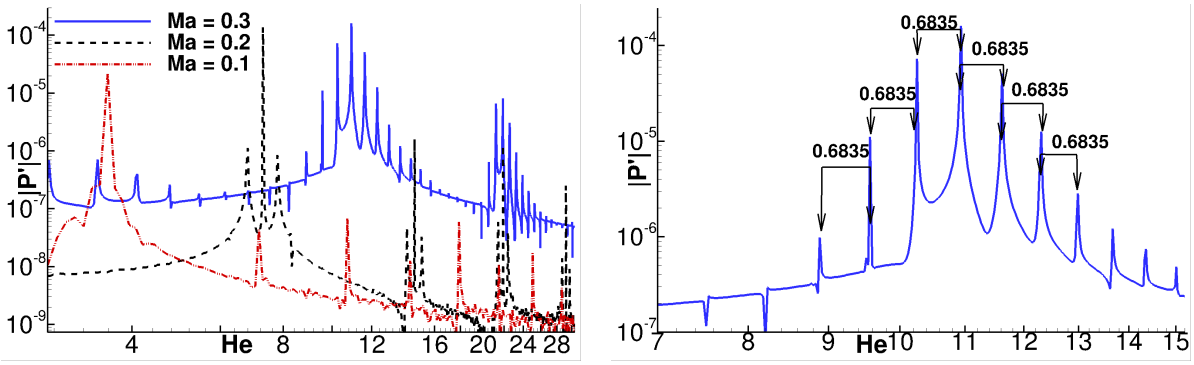

Figure 3. Near-field pressure spectra for TE1, AoA = 0 deg. and $Re = 100000$. Left: $Ma = 0.1$, 0.2 and 0.3. Right: Detail of the tonal peak separation for $Ma = 0.3$.

where x_n is the coordinate for which the wave becomes unstable for each frequency ω. The black contour divides the unstable and stable regions. The results show that convective instability is present in the aft part of the airfoil for a wide range of frequencies, for the airfoil geometry TE1. The peak amplification and the frequency for which it occurs increases with both Reynolds and Mach numbers. The growth rate is increased as the adverse pressure gradient increases towards the trailing edge, due to the appearance first of an inflection point and second of boundary layer separation. However, total amplification is relatively small for most of the cases considered, attaining values above $N_{max} = 5$ only for $Re = 100000$ and $Ma = 0.2$ and 0.3. Calculations for the airfoil geometry TE2 only recover disturbance wave growth at the trailing edge, but due to the rounded nature of the TE, the weakly non-parallel assumption is not valid there and the results are considered not physical. The peak amplifications N_{max} and frequencies for which they occur ω_{max} are also shown in table 1 for some flow configurations. Dominant frequencies are found to be comparable to those corresponding to the global oscillator in the wake and the dominant ones in the near-field pressure spectra from the DNS.

3.3 A global instability mechanism?

The previous analyses show a very good agreement between the leading frequencies recovered in the DNS, that were associated with the vortex shedding at the wake, with the predictions of the global oscillator analysis. In most cases, these frequencies also lie in the range of the most amplified convective waves forming in the adverse-pressure-gradient boundary layer, even though this convective instability does not have the potential to sustain itself in the absence of other means of excitation. However, a series of tonal peaks appear in the DNS near-field pressure spectra as the Reynolds and Mach numbers are increased. These peaks exhibit a constant frequency separation for each flow conditions, peaking in amplitude around the frequencies associated to the wake vortex shedding and its harmonics (see figure 3).

Its has been suggested in the literature that this tonal peaks can be the result of a global instability, established by the feedback between the boundary-layer structures originated by the convective instability and the trailing edge. This can occur in different manners: (i) an absolute instability exists in the separated shear layer, close to the trailing edge, that creates a global oscillator within the boundary layer. The frequency due to this oscillator is different from that of the wake, and the difference between the two gives rise to a beating interaction producing the evenly separated frequencies. (ii) The vortical structures generated by the convective boundary-layer instability generate acoustic waves as they pass close to the trailing edge. Part of this acoustic radiation is radiated up-chord, and through a complex receptivity process, it excites new boundary-layer instabilities. (iii) The Kutta condition at the trailing edge imposes an adaptation of the complete flowfield on account of the vortical structures that are generated by the wake and separated shear layer. This adaptation, even if small in amplitude, modulates the underlying flow conditions and the instability properties.

Linear local or weakly-nonlocal (parabolized) analysis methodologies are in general not sufficient to study physical global instabilities, as ellipticity, non-linear and feedback effects are not taken into account. However, some information can still be gathered from the analysis. Mechanism (i) cannot be active, as the absolute instability of reversed-flow boundary-layer profiles requires of peak negative velocities larger than 15% of the free-stream velocity (Diwan (2009); Rodríguez *et al.* (2013)), much larger than the ones present in the configurations studied here.

Mechanism (ii) has been widely studied in the literature considering both DNS and experiments, and its existence and dominance is well founded today. The convective amplification analysis done in the previous section using PSE models adequately the boundary-layer instability, but the conversion to acoustic waves and especially the receptivity process that leads to the acoustic feedback are still open questions. The most controversial point found in the literature seems to be the receptivity process and the spatial region in which it is relevant.

Here, we study whether a feedback model based on localized receptivity can predict the tonal peaks. A localized receptivity model, as considered in the classic Rossiter's mechanism for open cavities, considers that the time required for

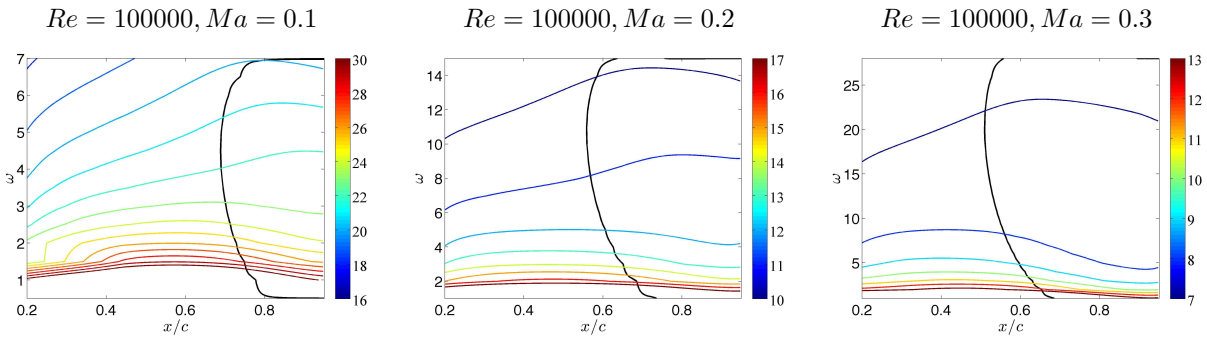

Figure 4. Colour: Contours of $P = t_c/t_a$ in the $x_R/c - \omega$ plane. Black: Neutral stability curve for boundary-layer instability. TE1 geometry at AoA = 0 deg., $Re = 100000$ (bottom) and $Ma = 0.1$ (left), 0.2 (middle) and 0.3 (right).

the acoustic propagation from the trailing edge to the receptivity point must be an integer multiple of the time required for the boundary-layer disturbances to propagate from the receptivity point to the trailing-edge. Acoustic waves propagate at the speed of sound ($c_\infty = 1$ in the dimensionless form used here), resulting in acoustic times $t_a \approx (x_{TE} - x_R)$, where x_{TE} is the coordinate of the trailing edge, x_R is the coordinate of the receptivity point, and the airfoil thickness is neglected as a first approximation. The convective time t_c is determined for each frequency using PSE results. For a fixed frequency ω, the phase velocity ω/α_r determines the propagation velocity of monochromatic instability waves, and the t_c is given by the quadrature

$$t_c = \frac{1}{\omega} \int_{x_R}^{x_{TE}} \alpha_r(X) \mathrm{d}X. \tag{7}$$

Literature suggests different locations for the localized receptivity coordinate x_R, including the leading edge, the suction peak, the boundary-layer separation location and, in connection with the e^N transition-prediction method, the frequency-dependent location where instability waves become unstable. If *any* localized x_R value is able to close the feedback loop, t_c must contain an integer number of acoustic times t_a. This possibility is analyzed visually in figure 4 for the TE1 geometry, AoA = 0 deg. and $Re = 100000$. The solid black line corresponds to the neutral curve of the boundary-layer instability. Color lines show the locations in the $x/c - \omega$ plane where $P = t_c/t_a$ is an integer number, and the color corresponds to the number P. The intersection of the P curves with a fixed x_R coordinate does not result into the evenly-spaced frequencies characteristic of the tonal peaks, nor it does the intersection with the stability neutral curve. Consequently, the localized receptivity model is inconsistent the tonal peaks.

Distributed receptivity models could still be applied to predict the tonal peak frequencies within mechanism (ii), but would require a more complex treatment of the receptivity-instability coupling. Mechanism (iii) is essentially global and elliptic, and its study requires the consideration of instability analyses based on the complete flow field and partial-derivative equations: a global eigenmode analysis.

3.4 Global eigenmode instability analysis

A global eigenmode analysis, considering the complete two-dimensional flow, has been developed in order to study mechanisms (ii) and (iii). A similar study was presented by Fosas de Pando *et al.* (2014), which suggested a possible explanation for the origin of the secondary tonal peaks.

Compared to the local and weakly non-parallel analyses discussed so far, global eigenmode analysis are much more involved in terms of complexity of the equations, computational implementation and memory and CPU time requirements. Considering a base flow fully dependent on the two dimensional space, eigenmodes must be allowed to have arbitrary spatial dependence on the same plane

$$\mathbf{q}(x, y, t) = \bar{\mathbf{q}}(x, y) + \varepsilon \hat{\mathbf{q}}(x, y) \exp(-\mathrm{i}\omega t) + c.c. \tag{8}$$

The set of governing equations used in the DNS, comprising the continuity, momentum and energy conservation equations in curvilinear coordinates as taken as the departure point in the derivation of the global eigenvalue problem. The equations are linearized with respect to the mean flow, and upon introduction of the modal form (8), results a generalized eigenvalue problem of the form

$$-\mathrm{i}\omega \mathbf{R}\hat{\mathbf{q}} = \mathbf{L}\hat{\mathbf{q}}, \tag{9}$$

where matrix operators $\mathbf{R}$ and $\mathbf{L}$ comprise first and second-order spatial derivatives, primitive and derivatives of the mean flow and the Reynolds, Mach and Prandtl numbers.

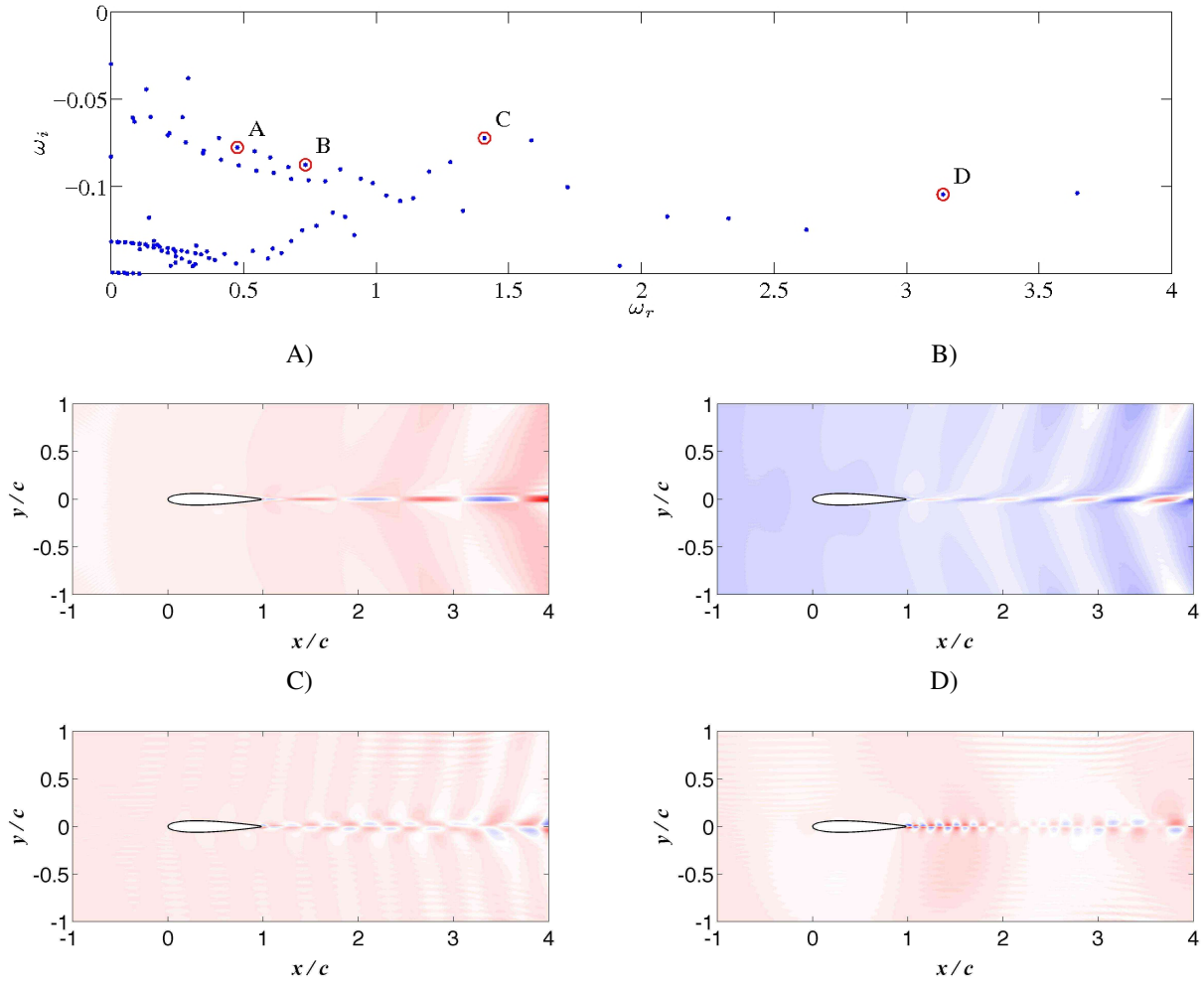

Figure 5. Top: Global eigenspectrum for TE1, AoA=0, $Re = 100000$, $Ma = 0.1$, and some selected eigenfunctions (A-D) highlighted in the eigenspectrum. The streamwise velocity component is shown.

The same O-type mesh from the DNS is also used in the stability analyses, preventing the appearance of numerical errors. A reduced domain is considered in the radial direction that extends over $8c$ on each direction; this is a value slightly larger than that used by Fosas de Pando *et al.* (2014). No-slip and isothermal boundary conditions are imposed at the airfoil surface. The treatment of the far-field boundary condition is problematic in compressible subsonic flows, as reflections of acoustic waves can contaminate the eigenfunctions. A sponge layer located between the outer boundary of the computational domain and a circle of radius equal to 6 and center at the trailing edge is used together with Dirichlet boundary conditions. Preliminary tests showed that this treatment reduced the contamination in the eigenfunctions by a large amount, but some reflections still exist towards the beginning of the sponge layer.

Figure 5 shows some representative results of the global eigenmode analysis for the airfoil geometry TE1 at AoA = 0 deg., $Re = 100000$ and $Ma = 0.1$. The top panel corresponds to the leading part of the eigenvalue spectrum, where ω_r is again the circular frequency and ω_i is the growth rate. All eigemodes were found to be stable, in disagreement with the wake oscillator analysis. This might be caused by lack of resolution in the present eigenmode computations, in spite of the 1000×620 mesh used. The streamwise velocity component of some selected eigenmodes, labeled A-B in the eigenspectrum are also shown in the figure. Modal fluctuations are localized in the wake region, and extend towards the domain boundary. For higher frequencies, oscillations of comparable amplitude emerge over the airfoil surface, accounting for boundary-layer instability waves.

4. CONCLUSIONS

Different methodologies for linear stability analysis have been employed in this paper in order to address the physical origin and prediction of tonal noise on airfoil at low-to-moderate Reynolds numbers and subsonic conditions. Two-dimensional direct numerical simulations of two modified NACA0012 airfoil geometries were considered. For some

combination of parameters, typically involving low Reynolds and Mach numbers, the near-field pressure spectra showed the presence of a tonal peak and its pure harmonics, whereas for higher Reynolds and Mach numbers a series of evenly-spaced secondary tones were found.

Weakly non-parallel stability analyses applied to the wake region predict a self-sustained global oscillator mechanism, responsible for the von Karman wake vortices, whose frequency matches closely that of the tonal peak in the simulations, and also that of the higher amplitude one when secondary tones are present. This finding confirms that at low Reynolds numbers, the sound is associated with the formation of spanwise-coherent vortices in the near-wake region.

The convective amplification of disturbance waves on the airfoil's boundary layer was studied by means of parabolized stability equations. Only configurations with AoA = 0 deg. were considered as the pressure and lee sides of the airfoil are approximately symmetric. Convective waves become unstable towards the aft portion of the airfoil, as the adverse-pressure-gradient and proximity to the round trailing edge result in boundary-layer separation. However, total amplifications are rather weak for most cases, attaining maximum N-factors below 5 for all cases analyzed except for the $Re = 100000$ and $Ma = 0.3$, in which it reached $N \approx 9$. Incidentally, most amplified frequencies are close to the ones corresponding to the wake instability. Consequently, fine-grained external turbulence is expected to generate small-amplitude instability waves that, upon reaching the separated shear layer, will give rise to spanwise rollers that will synchronize with wake oscillations.

Neither the wake oscillator nor the convective boundary-layer instability suffice to explain the origin of the secondary tones. Different global stability scenarios have been proposed in the literature. A direct feedback between the convective instability and acoustic radiation from the trailing edge, closed by a localized receptivity, was studied using parabolized stability equations herein, without success. The suggested reason for the lack of a favorable comparison with DNS frequencies is that, assuming that the feedback process exist, the receptivity process is not localized but distributed. With the objective of further pursuing a linear-stability-based explanation to this instability, a global eigenmode analysis was developed. Deeper analysis on the physics are underway.

5. ACKNOWLEDGEMENTS

The authors acknowledge the financial support of the Brazilian National Council of Scientific Research (CNPq) grants 405144/2016-4, 305512/2016-1, 423846/2016-7, and the São Paulo State Research Foundation (FAPESP) grants 2013/03413-4, 2014/24782-0, 2014/24782-0, 2017/01586-0.

6. REFERENCES

Arbey, H. and Bataille, J., 1983. "Noise generated by airfoil profiles placed in a uniform laminar flow". *Journal of Fluid Mechanics*, Vol. 134, pp. 33–47. ISSN 1469-7645.

Arias-Ramirez, W. and Wolf, W., 2015. "The effects of suction and blowing on tonal noise generation by blunt trailing edges". In *Proceedings of the 21st AIAA/CEAS Aeroacoustics Conference*. Dallas, Texas.

Arias-Ramirez, W. and Wolf, W.R., 2016. "Effects of trailing edge bluntness on airfoil tonal noise at low reynolds numbers". *Journal of the Brazilian Society of Mechanical Sciences and Engineering*, Vol. 38, pp. 2369–2380. ISSN 1678-5878.

Beam, R. and Warming, R., 1978. "An implicit factored scheme for the compressible Navier-Stokes equations". *AIAA Journal*, Vol. 16, No. 4, pp. 393–402. ISSN 0001-1452.

Bertolotti, F.P., Herbert, T. and Spalart, P., 1992. "Linear and nonlinear stability of the blasius boundary layer". *J. Fluid Mech.*, Vol. 242, pp. 441–474.

Brooks, T.F., Pope, D.S. and Marcolini, M.A., 1989. "Airfoil self-noise and prediction". Technical report, NASA.

Chomaz, J., Huerre, P. and Redekopp, L.G., 1988. "Bifurcation to local and global modes in spatially developing flows." *Phys. Rev. Lett.*, Vol. 60, pp. 25–28.

Chong, T.P. and Joseph, P.F., 2013. "An experimental study of airfoil instability tonal noise with trailing edge serrations". *Journal of Sound and Vibration*, Vol. 332, No. 24, pp. 6335 – 6358. ISSN 0022-460X.

Clark, L.T., 1971. "The radiation of sound from an airfoil immersed in a laminar flow". *Journal of Engineering for Gas Turbines and Power*, Vol. 93, No. 4, pp. 366–376. ISSN 0742-4795.

Desquesnes, G., Terracol, M. and Sagaut, P., 2007. "Numerical investigation of the tone noise mechanism over laminar airfoils". *Journal of Fluid Mechanics*, Vol. 591, pp. 155–182. ISSN 1469-7645.

Diwan, S.S., 2009. *Dynamics of Early Stages of Transition in a Laminar Separation Bubble*. Ph.D. thesis, Indian Institute of Science, Bangalore, India.

Ffowcs Williams, J.E. and Hawkings, D.L., 1969. "Sound generation by turbulence and surfaces in arbitrary motion". *Philosophical Transactions of the Royal Society of London. Series A, Mathematical and Physical Sciences*, Vol. 264, No. 1151, pp. pp. 321–342. ISSN 00804614.

Fink, M.R., 1975. "Prediction of airfoil tone frequencies". *Journal of Aircraft*, Vol. 12, No. 2, pp. 118–120. ISSN 0021-8669.

Fink, M., Schlinker, R. and Amiet, R., 1976. "Prediction of rotating-blade vortex noise from noise of non-rotating blades". Technical report, NASA.

Fosas de Pando, M., Schmid, P.J. and Sipp, D., 2014. "A global analysis of tonal noise in flows around aerofoils". *J. Fluid Mech.*, Vol. 754, pp. 5–38.

Herbert, T., 1997. "Parabolized stability equations". *Ann. Rev. of Fluid Mechanics*, Vol. 29, pp. 245–283.

Hersh, A. and Hayden, R., 1971. "Aerodynamics sound radiation from lifting surfaces with and without leading edge serrations". Technical report, NASA.

Huerre, P. and Monkewitz, P., 1990. "Local and global instabilities in spatially developing flows". *Ann. Rev. of Fluid Mechanics*, Vol. 22, pp. 473–537.

Jones, L.E. and Sandberg, R.D., 2011. "Numerical analysis of tonal aerofoil self-noise and acoustic feedback-loops". *J. Sound Vib.*, Vol. 330, pp. 6137–6152.

Kurotaki, T., Sumi, T., Atobe, T. and Hiyamae, J., 2008. "Numerical simulation around NACA0015 with tonal noise generation". In *46th AIAA Aerospace Sciences Meeting and Exhibit*. pp. 1–16.

Longhouse, R., 1977. "Vortex shedding noise of low tip speed, axial flow fans". *Journal of Sound and Vibration*, Vol. 53, No. 1, pp. 25–46. ISSN 0022-460X.

Nagarajan, S., Lele, S.K. and Ferziger, J.H., 2003. "A robust high-order compact method for large eddy simulation". *Journal of Computational Physics*, Vol. 191, No. 2, pp. 392–419. ISSN 0021-9991.

Paterson, R., Vogt, P., Fink, M. and Munch, C., 1973. "Vortex noise of isolated airfoils". *Journal of Aircraft*, Vol. 10, pp. 296–302.

Plogmann, B., Herrig, A. and Würz, W., 2013. "Experimental investigations of a trailing edge noise feedback mechanism on a NACA0012 airfoil". *Experiments in Fluids*, Vol. 54, No. 5, 1480. ISSN 0723-4864.

Rodríguez, D., Gennaro, E.M. and Juniper, M.P., 2013. "The two classes of primary modal instability in laminar separation bubbles". *J. Fluid Mech.*, Vol. 734, p. R4.

Smith, D., Paxson, R., Talmadge, R. and Hotzo, E., 1970. "Measurements of the radiated noise from sailplanes". Technical report, US Air Force Flight Dynamics Laboratory.

Tam, C.K.W. and Ju, H., 2011. "Aerofoil tones at moderate reynolds number". *J. Fluid Mech.*, Vol. 690, pp. 536–570.

Tam, C.K.W., 1974. "Discrete tones of isolated airfoils". *The Journal of the Acoustical Society of America*, Vol. 55, No. 6, pp. 1173–1177.

Wolf, W.R., Azevedo, J.L.F. and Lele, S.K., 2012a. "Convective effects and the role of quadrupole sources for aerofoil aeroacoustics". *Journal of Fluid Mechanics*, Vol. 708, pp. 502–538. ISSN 1469-7645.

Wolf, W.R., Azevedo, J.L.F. and Lele, S.K., 2013. "Effects of mean flow convection, quadrupole sources and vortex shedding on airfoil overall sound pressure level". *Journal of Sound and Vibration*, Vol. 332, pp. 6905–6912.

Wolf, W.R., Lele, S.K., Jothiprasard, G. and Cheung, L., 2012b. "Investigation of noise generated by a DU96 airfoil". In *18th AIAA/CEAS Aeroacoustics Conference (33th AIAA Aeroacoustics Conference)*. pp. 1–15.

7. RESPONSIBILITY NOTICE

The following text, properly adapted to the number of authors, must be included in the last section of the paper: The author(s) is (are) the only responsible for the printed material included in this paper.